

See discussions, stats, and author profiles for this publication at: <https://www.researchgate.net/publication/46179684>

# Unusual, Solvent Viscosity-Controlled Tautomerism and Photophysics: Meso-Alkylated Porphycenes

ARTICLE in JOURNAL OF THE AMERICAN CHEMICAL SOCIETY · SEPTEMBER 2010

Impact Factor: 12.11 · DOI: 10.1021/ja105353m · Source: PubMed

CITATIONS

28

READS

61

11 AUTHORS, INCLUDING:



**Michał Gil**

Instytut Chemii Fizycznej PAN

30 PUBLICATIONS 524 CITATIONS

SEE PROFILE



**Czesław Radzewicz**

University of Warsaw

95 PUBLICATIONS 1,333 CITATIONS

SEE PROFILE



**Paweł Borowicz**

Institute of Electron Technology

55 PUBLICATIONS 622 CITATIONS

SEE PROFILE



**J. Waluk**

Polish Academy of Sciences

257 PUBLICATIONS 3,690 CITATIONS

SEE PROFILE

### Unusual, Solvent Viscosity-Controlled Tautomerism and Photophysics: *Meso*-Alkylated Porphycenes

Michał Gil,<sup>†</sup> Jacek Dobkowski,<sup>†</sup> Gabriela Wiosna-Sałyga,<sup>†</sup> Natalia Urbańska,<sup>†</sup> Piotr Fita,<sup>‡</sup> Czesław Radzewicz,<sup>†,‡</sup> Marek Pietraszkiewicz,<sup>†</sup> Paweł Borowicz,<sup>†</sup> David Marks,<sup>§</sup> Max Glasbeek,<sup>§</sup> and Jacek Waluk<sup>\*,†</sup>

*Institute of Physical Chemistry, Polish Academy of Sciences, Kasprzaka 44/52, 01-224 Warsaw, Poland, Institute of Experimental Physics, University of Warsaw, Hoża 69, 00-681 Warsaw, Poland, and Laboratory for Physical Chemistry, University of Amsterdam, Nieuwe Achtergracht 129, 1018 WS Amsterdam, The Netherlands*

Received June 24, 2010; E-mail: waluk@ichf.edu.pl

**Abstract:** Stationary and time-resolved studies of 9,10,19,20-tetramethylporphycene and 9,10,19,20-tetra-*n*-propylporphycene in condensed phases reveal the coexistence of *trans* and *cis* tautomeric forms. Two *cis* configurations, *cis*-1 and *cis*-2, play a crucial role in understanding the excited-state deactivation and tautomer conversion dynamics. The *trans*–*trans* tautomerization, involving intramolecular transfer of two hydrogen atoms, is extremely rapid ( $k \geq 10^{13} \text{ s}^{-1}$ ), both in the ground and lowest electronically excited states. The *cis*-1–*trans* conversion rate, even though the process is thermodynamically more favorable, is much slower and solvent-dependent. This is explained by the coupling of alkyl group rotation with the hydrogen motion. Excited-state deactivation is controlled by solvent viscosity: the  $S_1$  depopulation rate decreases by more than 2 orders of magnitude when the chromophore is transferred from a low-viscosity solution to a polymer film. Such behavior confirms a model for excited state deactivation in porphycene, which postulates that a conical intersection exists along the single hydrogen transfer path leading from the *trans* to a high energy *cis*-2 tautomeric form. For this process, the tautomerization coordinate includes not only hydrogen translocation but also large-amplitude twisting of the two protonated pyrrole moieties attached to the opposite sides of the ethylene bridge.

#### 1. Introduction

Synthesis of porphycene (Pc),<sup>1</sup> a constitutional isomer of porphyrin, was followed by numerous works dealing with characterization of the fundamental properties, such as structure, spectra, tautomerism, as well as possible applications.<sup>2–9</sup> The geometry of porphycene, comprising a rectangular cavity composed of four nitrogen atoms linked by two strong hydrogen bonds (Scheme 1), makes this molecule particularly attractive for studies of cooperativity in intramolecular hydrogen bonds,

tautomeric equilibria, and intramolecular double hydrogen transfer. Coherent, mode-specific tunneling of two internal protons has been discovered for Pc isolated in supersonic jets<sup>10,11</sup> and helium nanodroplets.<sup>12</sup> Tautomerization in Pc and its derivatives has been extensively studied in condensed phases,<sup>6,13–28</sup> both in

<sup>†</sup> Polish Academy of Sciences.

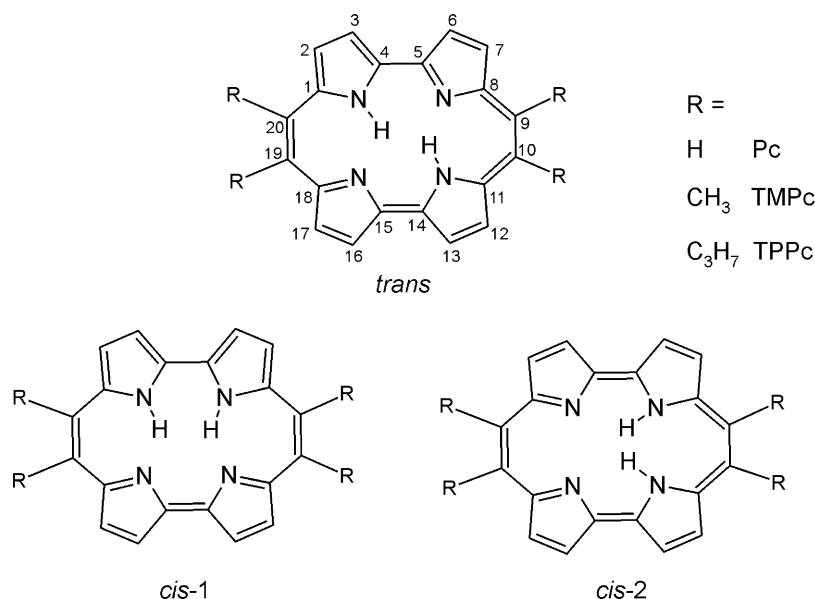
<sup>‡</sup> University of Warsaw.

<sup>§</sup> University of Amsterdam.

- (1) Vogel, E.; Köcher, M.; Schmickler, H.; Lex, J. *Angew. Chem., Int. Ed. Engl.* **1986**, *25*, 257.
- (2) Sánchez-García, D.; Sessler, J. L. *Chem. Soc. Rev.* **2008**, *37*, 215.
- (3) Sessler, J. L.; Gebauer, A.; Vogel, E. In *The Porphyrin Handbook*; Kadish, K. M., Smith, K. M., Guillard, R., Eds.; Academic Press: New York, 2000; Vol. 2, p 1.
- (4) Sessler, J. L.; Weghorn, S. J. *Expanded, Contracted & Isomeric Porphyrins*; Elsevier: Oxford, 1997.
- (5) Vogel, E. *Pure Appl. Chem.* **1996**, *68*, 1355.
- (6) Waluk, J.; Müller, M.; Swiderek, P.; Köcher, M.; Vogel, E.; Hohlneicher, G.; Michl, J. *J. Am. Chem. Soc.* **1991**, *113*, 5511.
- (7) Braslavsky, S. E.; Müller, M.; Mártire, D. O.; Pörting, S.; Bertolotti, S. G.; Chakravorty, S.; Koç-Weier, G.; Knipp, B.; Schaffner, K. J. *Photochem. Photobiol. B: Biol.* **1997**, *40*, 191.
- (8) Rubio, N.; Prat, F.; Bou, N.; Borrell, J. I.; Teixidó, J.; Villanueva, A.; Juarranz, A.; Cañete, M.; Stockert, J. C.; Nonell, S. *New J. Chem.* **2005**, *29*, 378.
- (9) Waluk, J. In *Handbook of Porphyrin Science*; Smith, K., Kadish, K., Guillard, R., Eds.; World Scientific: River Edge, NJ, 2010.

- (10) Sepioł, J.; Stepanenko, Y.; Vdovin, A.; Mordziński, A.; Vogel, E.; Waluk, J. *Chem. Phys. Lett.* **1998**, *296*, 549.
- (11) Vdovin, A.; Sepioł, J.; Urbańska, N.; Pietraszkiewicz, M.; Mordziński, A.; Waluk, J. *J. Am. Chem. Soc.* **2006**, *128*, 2577.
- (12) Vdovin, A.; Waluk, J.; Dick, B.; Slenczka, A. *ChemPhysChem* **2009**, *10*, 761.
- (13) Wehrle, B.; Limbach, H. H.; Köcher, M.; Ermer, O.; Vogel, E. *Angew. Chem., Int. Ed. Engl.* **1987**, *26*, 934.
- (14) Frydman, B.; Fernandez, C. O.; Vogel, E. *J. Org. Chem.* **1998**, *63*, 9385.
- (15) Langer, U.; Hoelger, C.; Wehrle, B.; Latanowicz, L.; Vogel, E.; Limbach, H. H. *J. Phys. Org. Chem.* **2000**, *13*, 23.
- (16) Lopez del Amo, J.; Langer, U.; Torres, V.; Pietrzak, M.; Buntowsky, G.; Vieth, H. M.; Shibl, M. F.; Kühn, O.; Bröring, M.; Limbach, H. H. *J. Phys. Chem. A* **2009**, *113*, 2193.
- (17) Waluk, J.; Vogel, E. *J. Phys. Chem.* **1994**, *98*, 4530.
- (18) Gil, M.; Jasny, J.; Vogel, E.; Waluk, J. *Chem. Phys. Lett.* **2000**, *323*, 534.
- (19) Gil, M.; Organero, J. A.; Waluk, J.; Douhal, A. *Chem. Phys. Lett.* **2006**, *422*, 142.
- (20) Waluk, J. *Acc. Chem. Res.* **2006**, *39*, 945.
- (21) Gil, M.; Waluk, J. *J. Am. Chem. Soc.* **2007**, *129*, 1335.
- (22) Pietrzak, M.; Shibl, M. F.; Bröring, M.; Kühn, O.; Limbach, H. H. *J. Am. Chem. Soc.* **2007**, *129*, 296.
- (23) Waluk, J. In *Hydrogen-Transfer Reactions*; Hynes, J. T., Klinman, J. P., Limbach, H. H., Schowen, R. L., Eds.; Wiley-VCH: Weinheim, 2007; Vol. 1, p 245.

Scheme 1



the ground and excited electronic states. The reaction has also been followed on the level of single porphycene molecules.<sup>29,30</sup> On the theoretical side, several papers discussed the energetics and dynamics of stepwise and concerted hydrogen transfer.<sup>31–36</sup>

With regard to applications, porphycene derivatives seem to be particularly attractive as potential phototherapeutic agents. In comparison with porphyrins, porphycenes exhibit a much stronger and red-shifted absorption in the visible region. Impressive phototherapeutic activity of various porphycenes has been reported in numerous papers.<sup>37</sup>

Besides strong absorption in the red part of the visible spectrum, a phototherapeutic agent should have a large triplet formation and singlet oxygen generation yields. While this is the case for many porphycenes, it seems that substitution at certain positions can strongly affect the photophysics, in particular the triplet formation efficiency. An intriguing behavior

has been reported for the 9,10,19,20-tetra-*n*-propylporphycene (TPPc).<sup>38</sup> Triplet formation in this molecule at room temperature is efficient when the triplet–triplet sensitization is used. However, for direct excitation into the singlet manifold, triplet population is negligible. This behavior suggests the presence of an efficient S<sub>1</sub>–S<sub>0</sub> internal conversion channel. We observed similar behavior for another *meso*-substituted derivative, 9,10,19,20-tetramethylporphycene (TMPc). Both TPPc and TMPc exhibit much weaker fluorescence than the parent, unsubstituted compound. Intense emission is recovered at low temperatures. We noted that the emission can be dramatically enhanced also at room temperature by placing the chromophore in a viscous environment. This observation, combined with the finding that the internal conversion involves internal hydrogen atoms, has led to a model for the origin of radiationless depopulation of the lowest excited singlet states in porphycenes.<sup>26</sup> According to this proposal, the deactivation involves crossing of the potential energy surfaces of the lowest excited and ground electronic states along a coordinate which combines (i) hydrogen transfer from the excited *trans*- to the *cis*-2 form (see Scheme 1) and (ii) distortion of the initially planar molecule toward a structure in which the two protonated pyrrole moieties are twisted in the opposite directions.

Differences between the parent compound and the *meso*-substituted porphycenes are also observed in the spectral patterns. The two lowest electronic transitions, separated by about 1000 cm<sup>−1</sup> in the parent compound, as well as in pyrrole-substituted alkyl derivatives, become red-shifted and very close-lying in *meso*-alkylated compounds.

Significant differences have also been found in the tautomerism involving the movement of two inner hydrogen atoms. Supersonic jet studies of Pc<sup>10</sup> show the presence of *trans* tautomers only, whereas the experiments performed for TPPc and TMPc<sup>11</sup> revealed the existence of two species, assigned to *trans*- and *cis*-1 structures, in agreement with calculations that predict nearly the same energies for these tautomers in TMPc.

In order to test the validity of the model for the radiationless depopulation, to understand the differences in the electronic

- (24) Fita, P.; Urbańska, N.; Radzewicz, C.; Waluk, J. *Z. Phys. Chem. Int. J. Res. Phys. Chem. Chem. Phys.* **2008**, *222*, 1165.
- (25) Fita, P.; Urbańska, N.; Radzewicz, C.; Waluk, J. *Chem.—Eur. J.* **2009**, *15*, 4851.
- (26) Sobolewski, A.; Gil, M.; Dobkowski, J.; Waluk, J. *J. Phys. Chem. A* **2009**, *113*, 7714.
- (27) Ghosh, A.; Moulder, J.; Bröring, M.; Vogel, E. *Angew. Chem., Int. Ed.* **2001**, *40*, 431.
- (28) Kay, C. W. M.; Gromadecki, U.; Törring, J. T.; Weber, S. *Mol. Phys.* **2001**, *99*, 1413.
- (29) Piwoński, H.; Stupperich, C.; Hartschuh, A.; Sepiół, J.; Meixner, A.; Waluk, J. *J. Am. Chem. Soc.* **2005**, *127*, 5302.
- (30) Piwoński, H.; Hartschuh, A.; Urbańska, N.; Pietraszkiewicz, M.; Sepiół, J.; Meixner, A.; Waluk, J. *J. Phys. Chem. C* **2009**, *113*, 11514.
- (31) Kozłowski, P. M.; Zgierski, M. Z.; Baker, J. *J. Chem. Phys.* **1998**, *109*, 5905.
- (32) Walewski, Ł.; Krachtus, D.; Fischer, S.; Smith, J. C.; Bala, P.; Lesyng, B. *Int. J. Quantum Chem.* **2006**, *106*, 636.
- (33) Shibl, M. F.; Pietrzak, M.; Limbach, H. H.; Kühn, O. *ChemPhysChem* **2007**, *8*, 315.
- (34) Smedarchina, Z.; Shibl, M. F.; Kühn, O.; Fernández-Ramoz, A. *Chem. Phys. Lett.* **2007**, *426*, 314.
- (35) Smedarchina, Z.; Siebrand, W.; Fernandez-Ramos, A.; Meana-Paneda, R. *Z. Phys. Chem. Int. J. Res. Phys. Chem. Chem. Phys.* **2008**, *222*, 1291.
- (36) Walewski, Ł.; Waluk, J.; Lesyng, B. *J. Phys. Chem. A* **2010**, *114*, 2313.
- (37) Stockert, J. C.; Cañete, M.; Juarranz, A.; Villanueva, A.; Horobin, R. W.; Borrell, J.; Teixidó, J.; Nonell, S. *Curr. Med. Chem.* **2007**, *14*, 997.

- (38) Levanon, H.; Toporowicz, M.; Ofir, H.; Fessenden, R. W.; Das, P. K.; Vogel, E.; Köcher, M.; Pramod, K. *J. Phys. Chem.* **1988**, *92*, 2429.

structure and spectra, to check for the presence of different tautomeric forms in condensed phases, and to analyze possible tautomerization mechanisms, we have carried out systematic spectral and photophysical studies of TMPc and TPPc in various environments, combined with quantum chemical calculations. The results, qualitatively similar for both compounds, demonstrate that alkyl substitution on the ethylene bridge brings about significant structural, spectral, and photophysical changes from the behavior of the parent compound. Two forms, assigned to *trans*- and *cis*-1 tautomers, are observed in condensed phases. The decay of both forms from  $S_1$  is crucially dependent on the viscosity of the environment. A surprising result is that the excited state *cis*-1-*trans* conversion is much slower than the *trans*-*trans* reaction and that it is controlled by viscosity. We propose a model which explains this rather unusual behavior. More specifically, the translocation of a single hydrogen atom is coupled to other molecular motions, whereas for the double hydrogen transfer this does not seem to be the case.

The observation that the lowest excited singlet state of *meso*-alkylated porphycenes is rapidly deactivated by internal conversion to the ground state, thus bypassing the triplet, can have important implications for phototherapy. Equally important is the finding that the rates of both deactivation and tautomerization can be controlled by the viscosity of the medium. It creates such possibilities as (i) more precise mapping of the chromophore, e.g., within the cells or (ii) using porphycenes as microviscosity reporters.

## 2. Experimental and Computational Details

The synthesis and purification of porphycenes were based on the procedures described in the literature.<sup>1,39,40</sup> The solvents included *n*-hexane (Uvasol, spectral grade), cyclohexane (CH, Merck, for spectroscopy), tetrahydrofuran (THF, Merck, LiChrosol), acetonitrile (ACN, Aldrich, spectrophotometric grade), dimethyl sulfoxide (DMSO, Uvasol, for spectroscopy), methanol (MeOH, Sigma-Aldrich, spectral grade), ethanol (EtOH, Merck, Uvasol, for fluorometry), diethyl ether (Merck, for spectroscopy), isopentane (Merck, for spectroscopy), liquid paraffin (Uvasol, for spectroscopy), poly(vinyl butyral-*co*-vinyl alcohol-*co*-vinyl acetate) (PVB, Aldrich, average molecular weight 90000–120000), poly(methyl methacrylate) (PMMA, Aldrich, 99%, medium molecular weight), and poly(vinyl alcohol) (Riedel-de Haën).

Various procedures were used for the preparation of polymer samples. PVB sheets were obtained by solving the polymer in THF, containing a small amount of the chromophore, and casting the solution on a Petri dish. Slow solvent evaporation was crucial for producing transparent films of good optical quality. A similar technique was applied for preparing PVA films; water was used as a solvent, with a small amount of alcohol solution of porphycene. PMMA samples were manufactured by polymerization of the monomer solution, containing the investigated chromophore, in an oil bath, slowly rising the temperature in the range of 313–363 K over a period of 4 days. Before polymerization, monomeric PMMA was distilled at a reduced pressure in order to remove the polymerization inhibitor. The samples were mechanically cut and polished to obtain disks of 25 mm diameter and a thickness of 0.3–1 mm.

Electronic absorption spectra were measured on a Shimadzu UV 3100 spectrophotometer equipped with a home-built temperature control chamber. Stationary fluorescence spectra were recorded on

an Edinburgh FS 900 CDT spectrofluorimeter. Variable-temperature emission and anisotropy measurements were performed on a compact Jasny spectrofluorometer.<sup>41</sup> For variable-temperature experiments involving polymer samples, the films were placed inside a closed-cycle Displex 202 helium cryostat.

Magnetic circular dichroism (MCD) spectra were recorded with an OLIS DSM 17 CD spectropolarimeter, equipped with a permanent magnet.

Fluorescence decays in the nanosecond range were measured on an Edinburgh Instruments FL900 spectrofluorometer. As pulsed excitation sources, nanosecond flash lamp or nano- and picosecond diodes (IBH NanoLEDs) were used, yielding 590 and 625 nm pulses of 1.5 ns duration or a 633 nm, 200 ps pulse. The NanoLEDs were also used in combination with Digikröm CM110 or CM112 monochromators, PicoQuant TimeHarp 100 PC-board for time-correlated single photon counting, and a Becker & Hickl PMC 100-4 photomultiplier.

For the analysis of subnanosecond fluorescence decays, a home-built setup was used, based on the excitation with Becker & Hickl BHL-600 picosecond diode laser module (635 nm, 100 ps pulse), RMS20X Olympus microscope objective, Digikröm CM110 monochromator, Becker & Hickl SPC-830 time-correlated single photon counting module, and an id100-20 id Quantique ultralow-noise single-photon detection module. The decay profiles were recorded over at least 4 orders of magnitude (usually with about 50000 counts at maximum). Particular attention was focused on a proper background level determination, as this was crucial for a reliable fitting of the biexponential decays with the components differing only by a factor of 2–3.

For experiments requiring temporal resolution of single picoseconds, a single photon counting setup described in detail elsewhere<sup>42</sup> was used, with the excitation wavelength set at 653 nm. The halfwidth of the excitation pulse was  $19 \pm 1$  ps. This setup was also applied for recording the decay of emission anisotropy.

Fluorescence decays were analyzed using the FAST Advanced Analysis of Fluorescence Kinetics software (Edinburgh Instruments, versions 2 and 3).

Transient absorption studies in the picosecond range were initially performed on a home-built instrument with 30 ps resolution.<sup>43</sup> Some of the measurements were then repeated using an improved setup that provided a temporal resolution better than 5 ps.<sup>44</sup>

The procedure of measuring temporal evolution of anisotropy using pump-and-probe technique with femtosecond time resolution has been described in detail elsewhere.<sup>24,25</sup> Briefly, a train of pulses from a noncollinear optical parametric amplifier (NOPA, Topas-white from Light Conversion) was split in order to obtain pump and probe beams. Both beams were linearly polarized, the polarization of the probe beam being rotated by 45° with respect to that of the pump. Two polarization components (parallel and perpendicular to the excitation) of the probe pulses were separated by a calcite polarizer and their intensity was measured by two photodiodes. The pump beam was periodically chopped using a mechanical shutter in order to measure optically induced changes of the absorbance of the sample, from which the transient absorption anisotropy was later calculated.

Ground-state geometry optimizations, as well as calculations of transition states, were done using density functional theory (DFT) with B3LYP functional and 6-31G(d,p) basis set. The same functional and basis set were applied for  $S_1$  geometry optimization and calculations of electronic transition energies by time-dependent density functional theory (TD-DFT). All of the calculations were done using Gaussian 03 and Gaussian 09 suites of programs. In

(41) Jasny, J.; Waluk, J. *Rev. Sci. Instrum.* **1998**, *69*, 2242.

(42) Proposito, P.; Marks, D.; Zhang, H.; Glasbeek, M. *J. Phys. Chem. A* **1998**, *102*, 8894.

(43) Dobkowski, J.; Grabowski, Z. R.; Jasny, J.; Zieliński, Z. *Acta Phys. Pol. A* **1995**, *88*, 455.

(44) Dobkowski, J.; Sazanovich, I. *Pol. J. Chem.* **2008**, *82*, 831.

(39) Vogel, E.; Köcher, M.; Lex, J.; Ermer, O. *Isr. J. Chem.* **1989**, *29*, 257.

(40) Urbańska, N.; Pietraszkiewicz, M.; Waluk, J. *J. Porphyrins Phthalocyanines* **2007**, *11*, 596.



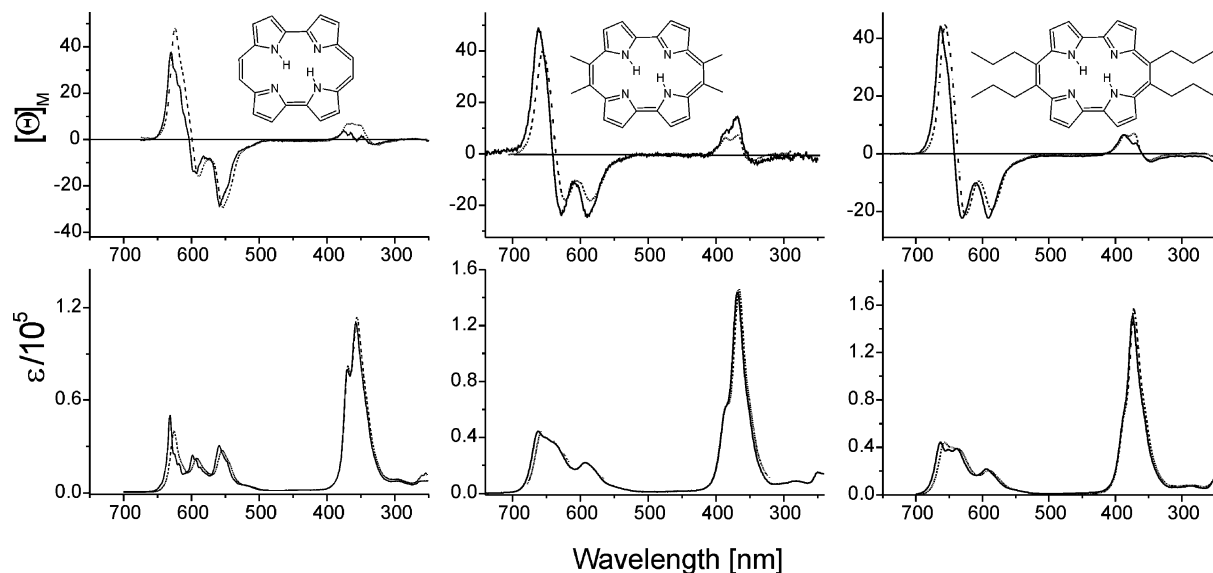


**Figure 1.** Bottom: absorption. Top: MCD spectra recorded at 293 K in *n*-hexane (solid line) and acetonitrile (dashed line).

the optimization procedure, the keywords Int=Tight and Grid=Ultrafine were used to enhance the calculation accuracy.

### 3. Results

#### 3.1. Stationary Electronic Absorption and MCD Spectra.

Figure 1 presents the comparison of electronic absorption and MCD spectra of the parent porphycene and two derivatives. The largest changes caused by alkyl substitution are observed in the low energy region. The transitions to  $S_1$  and  $S_2$ , separated by about  $1000\text{ cm}^{-1}$  in Pc,<sup>45</sup> lie closer to each other in both TPPc and TMPc. Linear dichroism (LD) studies of TPPc embedded in polyethylene sheets resulted in the value of  $600\text{ cm}^{-1}$  for the  $S_1$ – $S_2$  energy gap.<sup>46</sup> The shape of the absorption suggests that no  $S_1$ – $S_2$  state inversion occurs upon alkyl substitution. This is in line with TD-DFT 6-31G(d,p) calculations, which yield the same dominant electronic configurations for the two lowest singlet excited states in Pc and TMPc: The  $S_0$ – $S_1$  transition is dominated by the second HOMO–LUMO electronic configuration, whereas the transition to  $S_2$  is dominated by the HOMO–LUMO promotion. The shape and ordering of the frontier  $\pi$  orbitals remains the same in the two compounds (Figure 1S, Supporting Information).

The LD studies of TMPc revealed that the  $S_0$ – $S_1$  transition moment forms a larger angle,  $43^\circ$ , with the horizontal molecular axis than the  $S_0$ – $S_2$  transition moment for which the value of  $27^\circ$  was obtained. The calculations for TMPc yield the values of  $40^\circ$  and  $36^\circ$ , respectively. For Pc, the corresponding values are  $51^\circ$  and  $38^\circ$ . This is illustrated in Figure 2, which also shows how the transition moment direction changes as a result of *trans*–*trans* tautomerization: the angle  $\alpha$  formed between the  $S_0$ – $S_1$  transition moments in the initial and final structures can be determined by polarization studies.

Both absorption and MCD spectra of TPPc and TMPc are very similar. The same  $-,+,-,+$  pattern of Faraday  $B$  terms is observed, expected for the so-called negative-hard chromophores, characterized by unequal splitting of two highest occupied and two lowest unoccupied  $\pi$  orbitals:  $\Delta\text{HOMO} \ll$

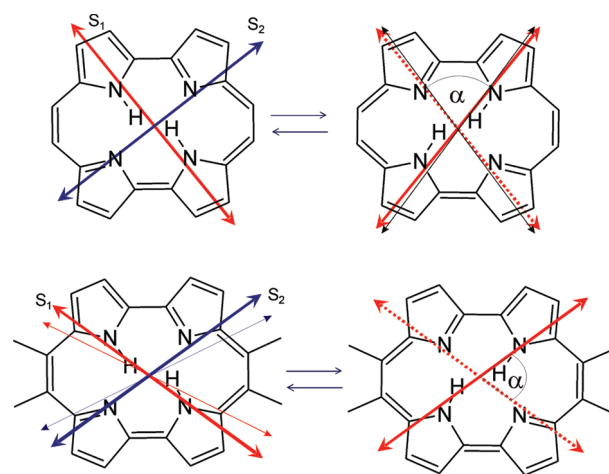


**Figure 2.**  $S_0$ – $S_1$  and  $S_0$ – $S_2$  transition moment directions, calculated for Pc and TMPc (solid lines). Right: the angle  $\alpha$  formed by the  $S_0$ – $S_1$  transition moments in the initial and final *trans* forms. Thin black arrows (top right) show the directions experimentally determined for Pc. Thin arrows (bottom left) indicate the directions determined for TPPc by LD studies.<sup>46</sup>

$\Delta\text{LUMO}$ .<sup>47</sup> This type of splitting also explains the MCD intensity pattern, which is different than that of the absorption. Contrary to the latter, the Soret bands are weaker than the Q transitions in the MCD spectra. A detailed analysis of MCD of porphycenes has been presented elsewhere.<sup>6</sup>

For all three compounds, only minor absorption changes are observed upon passing from a nonpolar to a polar solvent. In principle, one could expect some changes for comparable contributions of *cis* and *trans* tautomers. By symmetry, the latter cannot have a permanent dipole moment, whereas the former can. The *cis* forms could then be preferentially stabilized in polar environments. However, closer analysis of the calculated transition energies and dipole moments shows that no significant solvatochromism should be expected. The transition energies calculated for the *trans* and *cis* species are very similar, in agreement with the results of supersonic jet studies,<sup>11</sup> which revealed a separation of only  $12.5$  and  $17\text{ cm}^{-1}$  for the  $0$ – $0$

(45) Starukhin, A.; Vogel, E.; Waluk, J. *J. Phys. Chem. A* **1998**, *102*, 9999.

(46) Birklund-Andersen, K.; Vogel, E.; Waluk, J. *Chem. Phys. Lett.* **1997**, *271*, 341.

(47) Michl, J. *Tetrahedron* **1984**, *40*, 3845.

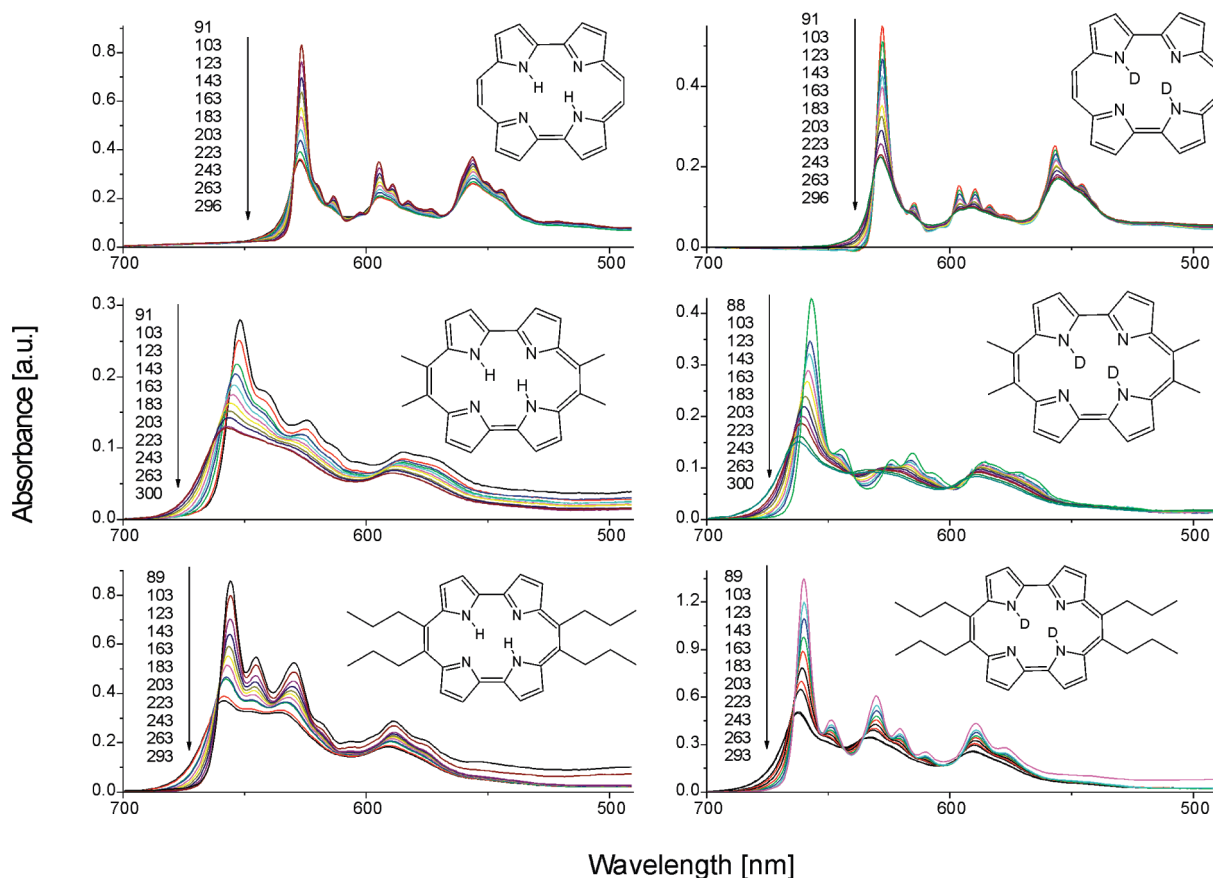


**Figure 3.** Temperature dependence of absorption, recorded for undeuterated (left, MeOH/EtOH 1:1 mixture) and N-deuterated species (right, MeOH/EtOH 1:1 mixture): top, Pc; middle, TMPc; bottom, TPPc. The arrows show the evolution of the intensities of the absorption maxima with increasing temperature (K).

transitions in the two tautomeric forms of TMPc and TPPc, respectively. A slight blue shift in the *cis* with respect to the *trans* form is calculated for the  $S_1 \leftarrow S_0$  transition ( $61\text{ cm}^{-1}$  and  $172\text{ cm}^{-1}$  for Pc and TMPc, respectively). For the  $S_2 \leftarrow S_0$  transition, even smaller shifts to the red are obtained ( $31\text{ cm}^{-1}$  and  $128\text{ cm}^{-1}$ ). Moreover, the predicted change of dipole moment after excitation to  $S_1$  is minor ( $1.17$  and  $1.22\text{ D}$  for Pc in  $S_0$  and  $S_1$ ; the corresponding values for TMPc are  $0.97$  and  $0.86\text{ D}$ ). Thus, the lack of significant spectral changes in the room temperature electronic absorption spectra in solvents of different polarity is not a strong argument for the absence of two tautomeric species. On the other hand, the time-resolved emission measurements, described below, clearly demonstrate the presence of two different forms.

An indication that more than one tautomeric form can be present in the *meso*-alkylated porphycenes is provided by comparison of the temperature dependence of the absorption spectra of the undeuterated species and the  $-d_2$  isotopomers, in which the inner protons have been replaced by deuterons (Figure 3). For parent Pc, the spectra of the two isotopomers are very similar. However, this is not the case for TPPc and TMPc. Whereas the spectra of  $-d_0$  and  $-d_2$  forms reveal similar spectral features, the relative intensities are very different. The same goes for the bandwidths, larger for the undeuterated species. These observations suggest a presence of comparable populations of the two tautomers in the undeuterated forms. In  $-d_2$  species, one form becomes dominant. The calculations for TMPc in the ground state predict a slight increase of the *cis*–*trans* energy difference in the  $-d_2$  versus the  $-d_0$  form,

$0.88$  and  $0.69\text{ kcal/mol}$ , respectively, indicating that the lower energy form, prevalent at low temperatures, corresponds to the *trans* tautomer. This conclusion is supported by fluorescence anisotropy measurements in low temperature alcohol glasses.<sup>17</sup> Depolarization of fluorescence was observed, caused by *trans*–*trans* tautomerization. If *cis* tautomers were dominant, no such effect would be expected.

**3.2. Stationary Fluorescence Spectra.** Figure 4 presents the temperature dependence of fluorescence spectra measured for undeuterated and doubly deuterated species in the temperature range from  $293\text{ K}$  down to about  $90\text{ K}$ . A spectacular difference is observed between the behavior of parent porphycene and the two *meso*-substituted derivatives. Fluorescence of porphycene, intense already at room temperature, becomes stronger at low temperature by a factor of less than two. On the other hand, the fluorescence of TMPc and TPPc in solutions is extremely weak at  $293\text{ K}$ . However, it increases dramatically at low temperatures, by nearly 3 orders of magnitude, which means that at low temperature the quantum yields of fluorescence are similar in all three derivatives. Deuteration of inner protons does not influence much the temperature dependence of the emission.

The activation energy of the process responsible for the temperature dependence of fluorescence was evaluated by plotting the logarithm of  $(1/\Phi - 1/\Phi_0)$  vs  $1/T$ ;  $\Phi$  denotes the fluorescence quantum yield, and  $\Phi_0$  is the maximum value, achieved at low temperatures: we assumed that  $\Phi = \Phi_0$  below  $90\text{ K}$ . This procedure yielded a value of  $2.7 \pm 0.2\text{ kcal/mol}$  for TPPc dissolved in 1:1 MeOH/EtOH mixture. A slightly larger value,  $3.3 \pm 0.2\text{ kcal/mol}$ , was obtained for TPPc- $d_2$ , measured

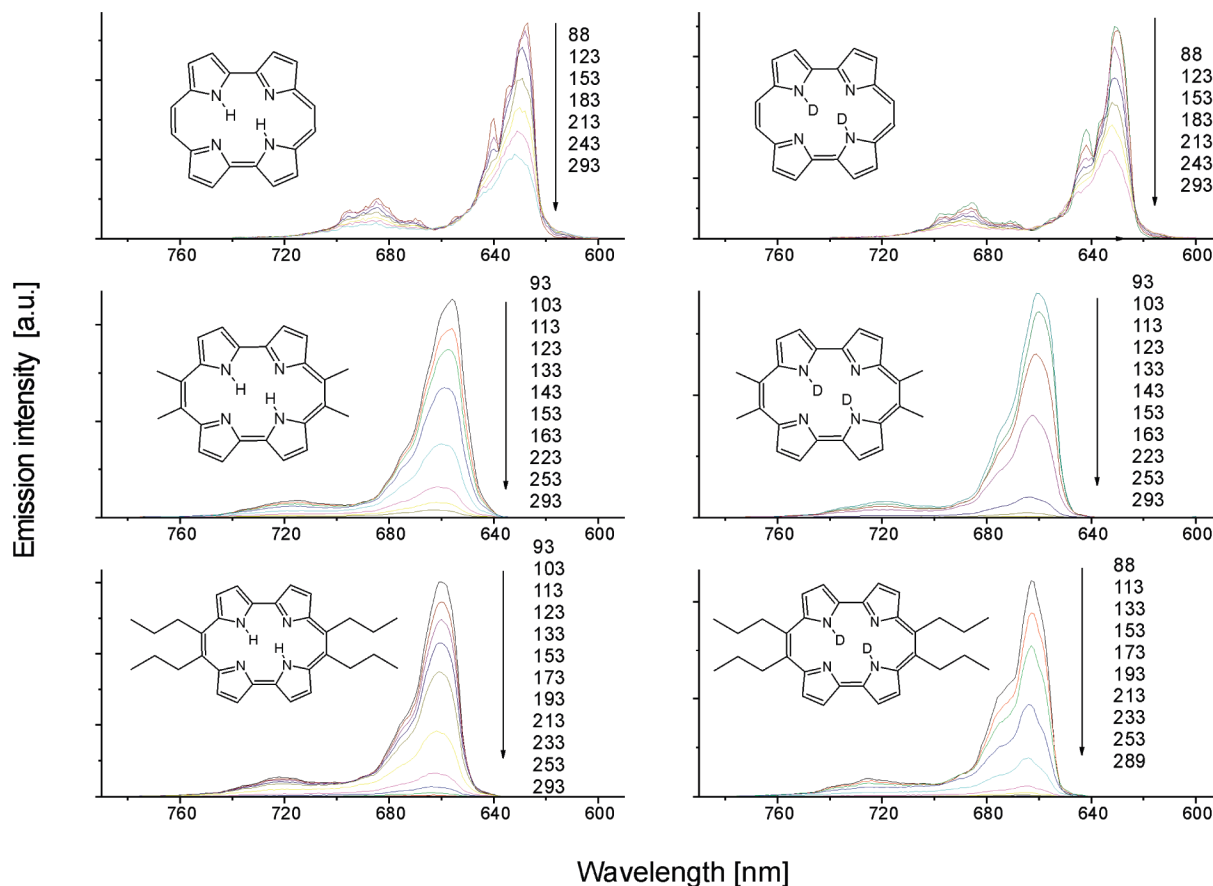


**Figure 4.** Temperature dependence of fluorescence, measured for undeuterated (left, MeOH/EtOH 1:1 mixture) and N-deuterated species (right, MeOD/EtOD 1:1 mixture): top, Pc; middle, TMPc; bottom, TPPc. The arrows show the evolution of the spectra with increasing temperature.

**Table 1.** Fluorescence Quantum Yields at 293 K

	solvent	$\Phi^a$
Pc	<i>n</i> -hexane	0.36
	toluene	0.36 <sup>b</sup>
	ACN	0.42
	DMSO	0.49
TMPc	<i>n</i> -hexane	$2.9 \times 10^{-4}$
	ACN	$3.2 \times 10^{-4}$
	BuOH	$6.0 \times 10^{-4}$
	DMSO	$1.5 \times 10^{-3}$
TPPc	<i>n</i> -hexane	$5.4 \times 10^{-4}$
	ACN	$8.1 \times 10^{-4}$
	MeOH	$5.2 \times 10^{-4}$
	DMSO	$3.5 \times 10^{-3}$

<sup>a</sup> Estimated accuracy:  $\pm 20\%$  for Pc,  $\pm 50\%$  for TMPc and TPPc.

<sup>b</sup> Reference 48.

in 1:1 MeOD/EtOD. The same procedure repeated for TMPc yielded the values of 3.3 and 3.6 kcal/mol for  $-d_0$  and  $-d_2$  forms, respectively.

The activation energy obtained for TPPc is the same as reported previously by Levanon et al.<sup>38</sup> for a solution in ethanol/toluene 1:1 mixture in a work devoted to triplet state formation of porphycenes. They obtained the values of  $2.7 \pm 0.5$  and  $3.2 \pm 0.5$  kcal/mol from the triplet–triplet absorption and fluorescence data, respectively.

Comparison of fluorescence intensities in different solvents (Table 1) shows that, contrary to the behavior of Pc, the quantum yields of *meso*-derivatives differ significantly for different environments. For instance, the fluorescence yields in nonpolar and nonviscous *n*-hexane and polar and nonviscous acetonitrile

are similar, but solving the chromophore in more viscous DMSO increases the emission intensity by a factor of 5. These observations suggest that it is the viscosity, not solvent polarity, which determines the radiative properties. We therefore extended the studies to much more viscous solvents and polymer films. Since the comparison of quantum yields at different temperatures in different media (solutions, glasses, polymers) is not very accurate, due to such factors as changing concentration, absorption, scattering from the films, etc., quantitatively more reliable data were provided by the analysis of time-resolved measurements.

**3.3. Time-Resolved Fluorescence and Transient Absorption Spectra.** The values of fluorescence decay times, obtained in various solvents at various temperatures (Table 2), confirm the differences between Pc on one hand, and the bridge-alkylated derivatives on the other. No large lifetime changes were detected for Pc in different environments, and only minor increase of the decay time at lower temperature was observed. In contrast, fluorescence decay times of TPPc and TMPc were found to depend dramatically on solvent and temperature, varying between the decays as short as a few picoseconds to values exceeding 10 ns. Most important, fluorescence decays were found to be biexponential, demonstrating the presence of two different forms. The amplitudes of the two decays are comparable at 293 K, with the longer decay having a larger contribution. At low temperatures, the longer-decaying component definitely prevails. Its contribution also becomes larger for the

(48) Aramendia, P. F.; Redmond, R. W.; Nonell, S.; Schuster, W.; Braslavsky, S. E.; Schaffner, K.; Vogel, E. *Photochem. Photobiol.* **1986**, *44*, 555.

**Table 2.** Fluorescence Decay Times

	solvent	T (K)	decay time(s) <sup>a</sup> (ns)	amplitudes ratio <sup>b</sup>
Pc	<i>n</i> -hexane	293	10.7	
	THF	293	11.7	
	ACN	293	12.0	
	MeOH	293	11.6 (11.8) <sup>c</sup>	
	MeOH/EtOH 1:1	293	11.4	
		77	14.3	
	MeOD/EtOD 1:1	77	23.0	
	PVA	293	12.9	
		24	15.9	
	PVB	293	12.8	
		130	13.3	
		110	13.4	
		90	13.4	
		75	13.5	
		60	13.4	
		45	13.3	
		15	14.3	
		8	14.0	
TMPc	THF	293	0.003/0.017 <sup>d</sup>	
	liquid paraffin	293	0.20/0.40	1.0
	PVB	293	0.5/2.3	0.30
		15	4.0/11.1	0.14
TPPc	CH	295	0.008/0.036	0.60
	THF	293	0.005/0.031 <sup>d</sup>	0.16 <sup>d</sup>
	ACN	295	0.006/0.030	0.63
	liquid paraffin	293	0.5/1.1	1.0
	PMMA	293	2.9/6.1	1.2
		77	4.3/9.6	0.20
		15	4.6/10.3	0.09
	PVB	293	1.2/3.2	0.25
	MeOH/EtOH 1:1	77	4.8/10.1	0.30
	MeOD/EtOD 1:1	77	6.5/12.7	0.09
	PrOH	133	3.3/6.3	0.39
		113	3.3/7.1	0.25

<sup>a</sup> Estimated accuracy:  $\pm 0.2$  ns for Pc,  $\pm 10\%$  for biexponential decays. <sup>b</sup> Estimated accuracy:  $\pm 50\%$ . <sup>c</sup> Reference 48. <sup>d</sup> Reference 19.

doubly deuterated species, as illustrated by the comparison of the data obtained from the decay of TPPc at 77 K in MeOH/EtOH and MeOD/EtOD mixtures. The longer/shorter decay amplitude ratio increases from 3.3 in the former to 11.4 for the latter. These results suggest that the longer-lived component should be attributed to the *trans* tautomeric form, while the shorter-lived should be attributed to the *cis*. Such assignment is corroborated not only by the prediction that the *trans* form is more stable but also because, according to calculations, deuteration increases the *cis*–*trans* energy difference. A definitive proof is provided by anisotropy measurements, discussed below.

A huge viscosity dependence of the fluorescence lifetimes parallels that observed for the quantum yields of TPPc and TMPc. For instance, the shorter and longer emission decay components increase for TPPc by factors of 100 and 35, respectively, upon passing from THF to a liquid paraffin solution. A further increase is observed for the chromophore embedded in PVB; now, the longer-lived component is more strongly affected. Actually, a much larger effect is caused by changing viscosity at 293 K than by lowering the temperature of an already viscous matrix. An example is provided by TPPc in PMMA: less than a 2-fold increase of both decay components is observed between 293 and 15 K.

Closer examination of Tables 1 and 2 reveals quantitative differences between TMPc and TPPc. Even though the same trends are observed, the values of quantum yields and fluorescence decays are, for the same solvent and the same temperature, significantly larger, approximately twice, for the *n*-propyl derivative. Since the electronic properties of the two molecules are very similar, as evidenced by the position of absorption and

fluorescence, the origin of different values of photophysical parameters, which are strongly viscosity-dependent, has to do with the presence of more bulky substituents in TPPc.

For TPPc, kinetics of the excited state decay was also studied by picosecond transient absorption spectroscopy. Because the spectral regions of excited and ground state absorption do not significantly overlap, it was possible to follow the temporary profile separately for ground state bleaching and  $S_1$ – $S_n$  signals (Figure 5). Because of lower temporal resolution, the biexponential character of the decay could not be resolved. However, the obtained decay times correlate well with the parameters extracted from fluorescence decay. For instance, for TPPc in acetonitrile at 293 K, a value of 21 ps, obtained from both excited state absorption and bleaching (Figure 5), corresponds to the average of biexponential decay components of 6 and 30 ps (Table 2).

The transient absorption experiments confirmed a large dependence of the excited state depopulation rate constants on viscosity and temperature. This is illustrated in Figure 5 by comparison of the decays recorded at 293 K in methanol and acetonitrile with the results obtained at 203 K in EPA (2:2:5 mixture of ethyl ether/isopentane/ethanol). For the latter, the excited state lifetime is an order of magnitude longer. Most important, the pump–probe experiments clearly demonstrate that the efficient radiationless process corresponds to  $S_0$ – $S_1$  internal conversion because the bleaching curve decays to zero. Thus, no population remains in a longer-lived triplet state. In this respect, the *meso* derivatives are different from parent porphycene, for which the triplet formation yield of about 40% has been reported.<sup>48,49</sup> However, at higher viscosity and/or lower temperature, the bleaching profile starts revealing a nonzero offset, indicating the formation of the triplet state. This observation indicates that the  $S_1$ – $T_1$  intersystem crossing rates are not much different in the three porphycenes.

Plotting the logarithm of the  $S_1$  lifetimes obtained from the transient signals against  $1/T$  yielded the value of the activation energy for  $S_0$ – $S_1$  internal conversion (Figure 6). Equal values were obtained for the solution of TPPc in EPA from transient absorption and bleaching profiles,  $2.6 \pm 0.3$  and  $2.5 \pm 0.3$  kcal/mol, respectively. These values are practically the same as  $2.7 \pm 0.2$  kcal/mol, obtained from stationary fluorescence measurement in MeOH/EtOH mixture.

**3.4. Anisotropy Studies.** Given the size of porphycenes, of which the molecular volume varies from about 860 Å<sup>3</sup> for Pc to 1400 Å<sup>3</sup> in TPPc, the rotational relaxation, and thus fluorescence depolarization, should occur in solution on the time scale ranging from about a hundred picoseconds to several nanoseconds. However, the experiment shows that it is not the case. Fluorescence anisotropy studies performed for room-temperature solutions of TPPc in acetonitrile and cyclohexane revealed a rapid decay of anisotropy, too fast to be quantitatively analyzed with picosecond resolution. In view of our previous investigations,<sup>17,21</sup> this result was not unexpected. Stationary fluorescence of parent porphycene, TPPc, and another alkyl derivative, 2,7,12,17-tetra-*n*-propylporphycene, was found to be depolarized even in low-temperature glasses: for excitation into  $S_1$ , instead of the value of 0.4, expected for the parallel directions of the absorption and emission transition moment directions, the experiment yielded the values slightly higher than 0.1 for Pc embedded in polymer films or organic glasses. The value

(49) Lament, B.; Karpiuk, J.; Waluk, J. *Photochem. Photobiol. Sci.* **2003**, *2*, 267.



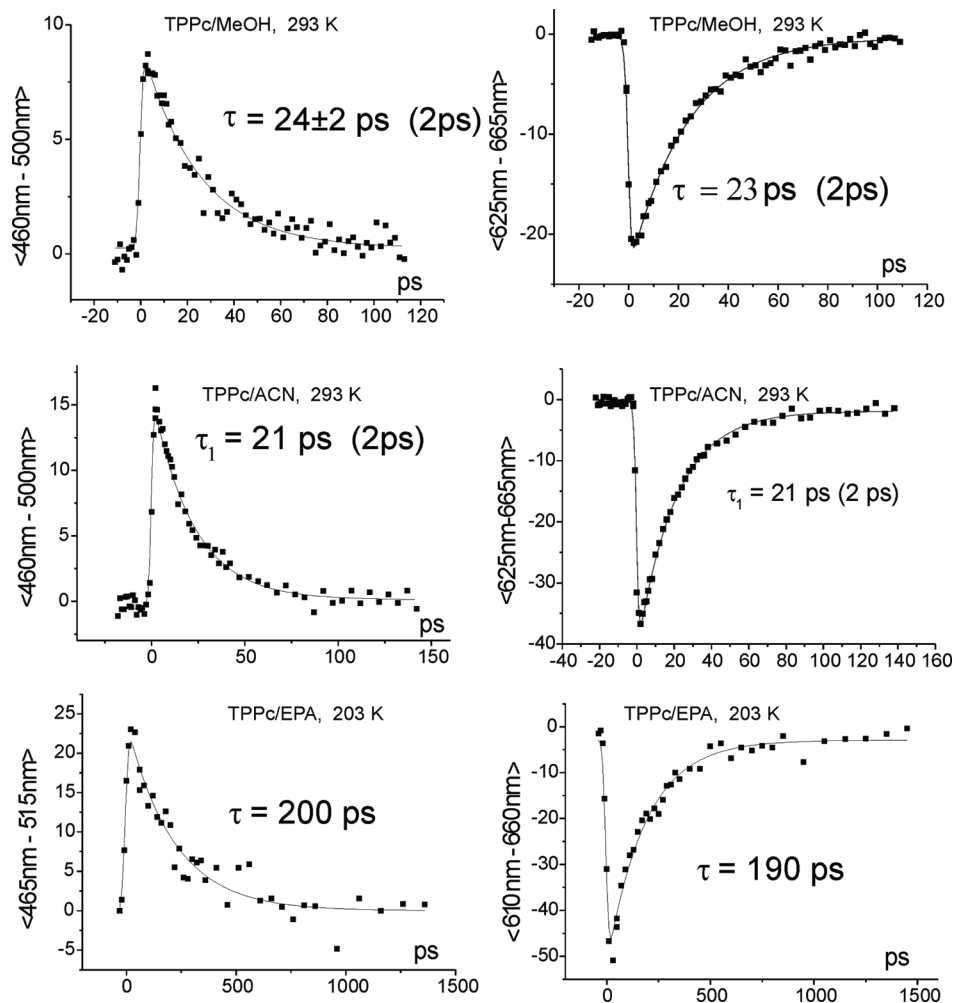


**Figure 5.** Kinetic profiles obtained from transient absorption (left) and ground-state bleaching (right) by plotting the pump–probe signal integrated over the spectral range indicated. From top to bottom: TPPc in MeOH (293 K), ACN (293 K), and EPA (203 K). The excitation wavelength was 352 nm.

approaching 0.4 could be recovered, however, by lowering the temperature below 10 K.<sup>21</sup> Fluorescence depolarization was interpreted as manifestation of the *trans*–*trans* tautomerization leading to the change in the transition moment directions, as illustrated in Figure 2. From the measured anisotropy values, the angle  $\alpha$  between the  $S_0$ – $S_1$  transition moment directions in the initially excited and tautomeric *trans* species could be evaluated. This methodology of studying tautomerization using polarized light has been extended to studies of single molecules of porphycene.<sup>29,30</sup> The same value of  $\alpha$ , the angle formed by  $S_0$ – $S_1$  transition moment directions was obtained as obtained previously from the bulk data. Finally, using polarized femto-second transient absorption spectroscopy, it was possible to monitor the reaction not only in the lowest excited singlet state, but also on the ground state level. This was done for Pc and four derivatives, including TMPc and TPPc.<sup>25</sup> Figure 7 presents the kinetic profiles of the anisotropy obtained at 293 K in two solvents of different viscosities. For porphycene in less viscous acetonitrile, two time scales of anisotropy decay are observed. A faster component decays in several picoseconds, whereas the other component is longer by about an order of magnitude. After about 100 ps, the anisotropy decays to zero. In a much more viscous ethylene glycol, the shorter component remains the same, but the longer one is no longer observed. Instead, a plateau is reached, with the anisotropy values of 0.12 for Pc, 0.18 for TMPc and 0.16 for TPPc. The shorter component is connected

with the depolarization due to *trans*–*trans* tautomerization, while the longer one, observed only in a less viscous solvent, is due to rotational diffusion.

One should note very different time scales for the anisotropy decay in Pc and the two alkyl derivatives. For the latter, the anisotropy drops much faster, to the value of 0.3, in less than 100 fs. This value is much shorter than either of the two fluorescence decay components. Such behavior is of fundamental importance for the mechanism of tautomerization in *meso*-alkylated porphycenes, discussed in the next section.

## 4. Discussion

**4.1. Detection of Different Tautomeric Forms.** Double-exponential decay of fluorescence observed for *meso*-alkylated porphycenes demonstrates the existence of two forms, which are assigned to *trans* and *cis*-1 tautomeric species. For parent porphycene, only the *trans* tautomer is observed. This is in accordance with B3LYP/6-31G(d,p) calculations, which predict for TMPc the energy difference between *cis*-1 and *trans* forms of only 1.40 kcal/mol, and even less, 0.69 kcal/mol, when the zero-point energy is included. For parent Pc, the corresponding numbers are 2.24 and 1.59 kcal/mol, respectively.

Both tautomeric forms have very similar electronic spectra. For TMPc isolated in a supersonic jet, the locations of the 0–0 transition differ by only 12 cm<sup>−1</sup>.<sup>11</sup> By symmetry, the *trans* form

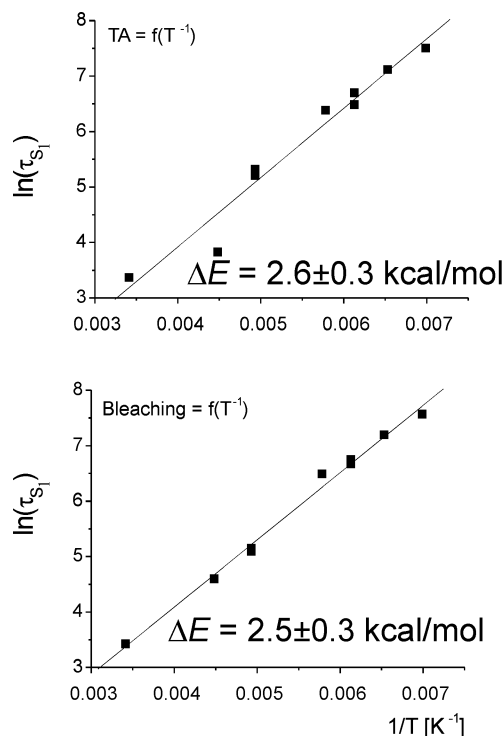


**Figure 6.** Plots of  $\ln(\tau)$  for  $S_1$  lifetimes obtained from integrated transient absorption (top) and bleaching (bottom) signals vs  $1/T$ , measured for TPPc in EPA. The integration limits were 465–515 nm for absorption and 610–660 nm for bleaching signals.

has no dipole moment, whereas the *cis* form does. However, since the changes of the dipole moment upon electronic excitation are minor, the absorption is weakly solvent-dependent.

Because of similar energies predicted for *trans* and *cis* isomers, it would be unsafe to assign the more stable form to the *trans* species solely on the basis of calculations. Fortunately, the deuteration effects discussed above and, especially, experiments which utilize polarized light provide strong arguments for such an assignment. The linear dichroism measurements carried out for TPPc embedded in stretched polyethylene films allowed determination of the orientation factors of the absorption transition moment directions; the obtained values range between 0.30 and 0.85.<sup>46</sup> The orientation factor is an average cosine square of the angle between the transition moment and the stretching direction. The symmetry of the *cis*-1 tautomer dictates that only two transition moment directions, vertical and horizontal with respect to the formula in Scheme 1, are possible for the in-plane polarized  $\pi\pi^*$  transitions. The largest value of the orientation factor,  $K_z$ , corresponds to the horizontally polarized transitions. It must be equal to or larger than 0.85, the largest value obtained experimentally. Because the three principal orientation factors,  $K_z$ ,  $K_y$ , and  $K_x$ , add up to 1, the value of  $K_y$ , corresponding to the vertically polarized transitions, must be smaller than 0.15; actually, one expects even a lower value, at most  $(1-0.85)/2$ . These possible values for  $K_z$  and  $K_y$  in the *cis* tautomer are completely different than the experimentally observed ones: 0.50 for the peaks at 15000 and 17000  $\text{cm}^{-1}$  and 0.70 for the peak at 15600  $\text{cm}^{-1}$ . The latter can thus be safely attributed to the *trans* tautomer, for which, owing to  $C_{2h}$  symmetry, any in-plane direction of the transition moment is allowed. The lower value of the orientation factor for the origin of the  $S_0$ – $S_1$  transition indicates that the corresponding transition moment forms a larger angle with the horizontal

axis than the moment of  $S_0$ – $S_2$  transition. This conclusion is confirmed by calculations, which yield 51° and 40° for the  $S_0$ – $S_1$  transition in Pc and TMPc, respectively. For the  $S_0$ – $S_2$  transition, the values of 38° and 36° are calculated (see Figure 2).

The second independent argument for the assignment of the *trans* structure as the dominant one comes from the anisotropy studies. Both fluorescence and transient absorption signals are partially depolarized under conditions where the molecular rotation is hindered. This is due to *trans*–*trans* tautomerization. The exchange of internal protons between the nitrogen atoms results in the reflection of transition moments in the vertical (or horizontal) plane, perpendicular to the plane of the chromophore (cf. Figure 2). The rate of the excited-state reaction can be determined from the values of fluorescence anisotropy.<sup>20,21</sup> Transient absorption and bleaching experiments allow to determine both ground and excited state reaction rates, depending on the selection of pump and probe wavelengths.<sup>25</sup> Moreover, the angle  $\alpha$  (Figure 2) between the  $S_0$ – $S_1$  transition moment directions in the two interconverting *trans* species can be determined. For porphycene, the value of  $74 \pm 3^\circ$  has been independently obtained from three different types of experiments: (i) fluorescence anisotropy studies;<sup>17,21</sup> (ii) transient absorption measurements;<sup>25</sup> (iii) analysis of spatial patterns of emission from single porphycene molecules.<sup>29,30</sup> The value of 74° corresponds to the anisotropy of 0.12 (observed, e.g., in the plateau reached in the transient anisotropy signal in a viscous solvent, Figure 7, bottom left). For TMPc, both fluorescence and pump–probe experiments reveal a higher value of 0.18 (Figure 7, top right). This can be interpreted in several ways. First, the  $S_0$ – $S_1$  transition moment direction in the *meso* derivatives may not be the same as in the parent molecule. The anisotropy of 0.18 can be obtained if the emission comes from two rapidly interconverting *trans* tautomers, of which the transition moments form an angle of 58°. Such an explanation is, however, highly unlikely. First, the calculations predict very similar angles in both Pc and TMPc, 78° and 80°; the reliability of these predictions could be verified by comparison with the experimental value of  $74 \pm 3^\circ$  established for Pc. Most important, the time-resolved studies show that both *trans* and *cis* species are present in  $S_1$ . Two decay times demonstrate that no equilibrium is established. On the other hand, rapid decay of anisotropy is observed, much faster than each of the fluorescence lifetimes. Such findings show that *trans*–*trans* tautomerization is extremely rapid ( $k > 10^{13} \text{ s}^{-1}$  for the reaction in  $S_0$  and  $k \approx 10^{13} \text{ s}^{-1}$  for the reaction in  $S_1$ ). The *cis*–*cis* conversion is probably also ultrafast, but this is not relevant for the anisotropy, because such reaction does not lead to a change in the transition moment direction.

Since for TMPc and TPPc both *trans* and *cis* tautomers are present, the measured stationary anisotropy value,  $r$ , reflects their contributions:  $r = f_{tr}r_{tr} + r_{cis}(1 - f_{tr})$ , where  $f_{tr}$  is the fraction of the *trans* tautomer. For the *cis* form,  $r_{cis} = 0.4$ . Assuming that  $r_{tr} = 0.12$ , as in Pc, results in  $f_{tr} = 0.79$ . In reality, the situation is more complicated. Some of the *trans* species are formed from *cis* ones. For those, the anisotropy is dictated by the angle between the  $S_0$ – $S_1$  transition moments in the *cis* and *trans* forms. The calculations predict that the lowest electronic transition in the *cis* tautomer of TMPc is vertically polarized, which corresponds to the angle of 50° and the anisotropy of 0.05. Taking into account the population of *trans* species excited via *cis* precursors would lower the value of  $f_{tr}$ . If the opposite were true, i.e., for the horizontally polarized  $S_0$ – $S_1$  transition in the

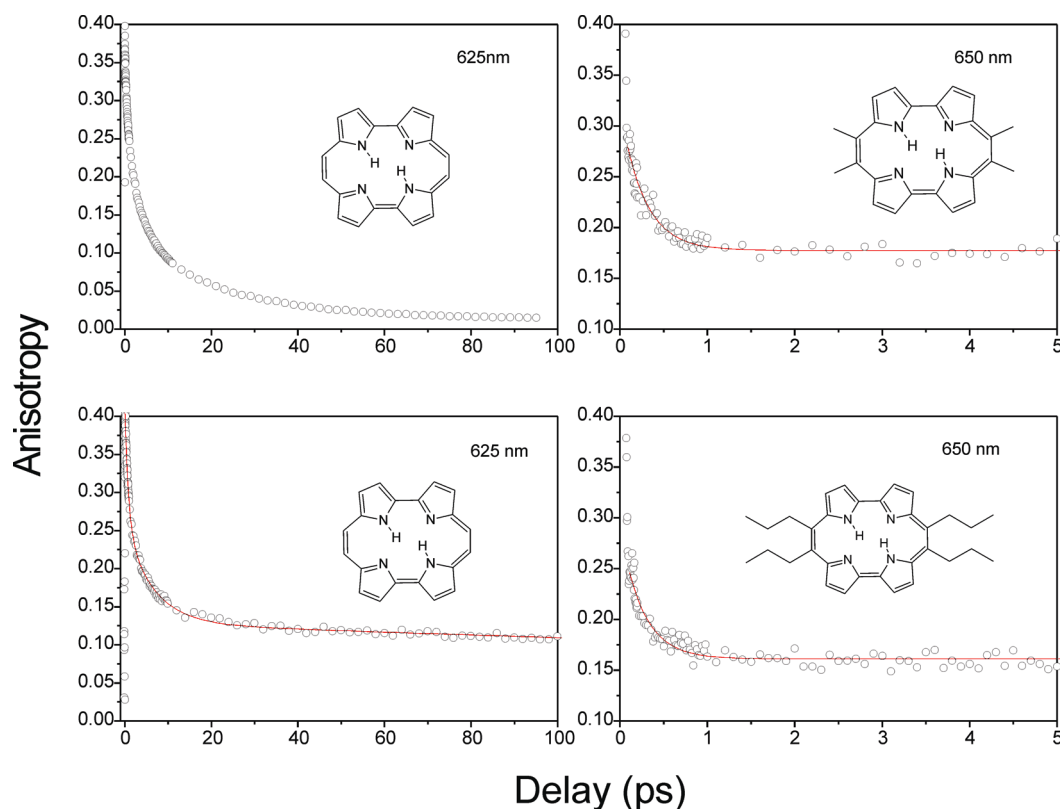


**Figure 7.** Anisotropy of the probe signal as a function of time delay from the pump pulse of the same wavelength. Top left: Pc in acetonitrile; bottom left, Pc in ethylene glycol. Right: TMPc (top) and TPPc (bottom) in mixtures of ethylene glycol and methanol. All spectra were measured at 293 K.

*cis* form, one would expect the angle of  $40^\circ$  and the anisotropy of 0.15. Then, a slightly higher  $f_{tr}$  value would be obtained.

The 1:4 ratio of *cis/trans* populations of TMPc and TPPc at 293 K corresponds to the energy difference of 0.80 kcal/mol, in perfect agreement with theoretical predictions. We also tried to estimate this ratio from the values of amplitudes obtained in the biexponential fittings of fluorescence decays at different temperatures (Table 2). Such a procedure, however, is not very accurate, as the values of amplitudes are quite sensitive to the fitting range; moreover, it assumes the same absorption spectra with the same absorption coefficients for the two tautomers. Still, the obtained values span a small range, from zero to a few tenths of a kcal/mol. It seems safe to conclude that the energy difference between *trans* and *cis* tautomers does not exceed 1 kcal/mol. In a polar environment, the difference may be even smaller, due to preferential stabilization of the *cis* form. The same pattern is predicted for both the ground and the lowest excited singlet state. The TD-DFT B3LYP/6-31G(d,p) optimization of *cis* and *trans* structures in  $S_1$  yield an energy difference of 1.25 kcal/mol; with ZPE correction, this value becomes 0.79.

**4.2. The Origin of Viscosity-Dependent Photophysics.** The rate of deactivation of the lowest excited singlet state in the two *meso*-derivatives can be 3 orders of magnitudes larger than that of the parent Pc at room temperature in low-viscosity solvents. At low temperatures, the difference disappears, as indicated by very similar fluorescence decay times of the three compounds in polymer films and alcohol glasses. Most spectacular is the change of photophysics of TMPc and TPPc at ambient temperature with solvent viscosity: The  $S_1$  depopulation occurs in picoseconds in nonviscous media, but it takes nanoseconds in polymers. A clear difference is observed between TMPc and TPPc: even though they both decay very

rapidly, in the same solvent the  $S_1$  deactivation of the latter is more than twice as long.

In the parent compound, efficient fluorescence is observed already at 293 K in nonviscous solvent. Lowering the temperature leads to only a slight increase in the emission quantum yield. One should note, however, a 60% longer fluorescence decay at 77 K after replacement of inner protons by deuterons (Table 1), indicating that the motion of inner protons plays a role in radiationless deactivation.

We have recently proposed a model for the radiationless deactivation of  $S_1$  in porphyrines<sup>26</sup> which can account for the observed differences between *meso*- and octaalkylated porphyrines on one hand and the parent compound and its 2,7,12,17-tetraalkyl- and 10,19-dimethyl derivatives on the other. The crucial species for this model is the *cis*-2 tautomer (Scheme 1). This structure lies so high in energy, about 2 eV, that it can be neglected in the analysis of ground-state tautomerization. This is, however, not the case for the excited state. According to calculations, the ground state of *cis*-2 has an open-shell character, whereas the closed-shell structure lies only slightly higher in energy. Along the *trans*–*cis*-2 hydrogen transfer coordinate, the open shell ground state of *cis*-2 tautomer correlates with the excited state of the *trans* tautomer, whereas the next electronic state, because of its closed-shell nature, with the ground state of the *trans* species. Such state ordering implies a crossing of ground- and excited-state potential energy surfaces along the *trans*–*cis*-2 excited-state hydrogen-transfer coordinate (Figure 8). A conical intersection along this coordinate provides an efficient channel of radiationless deactivation. Because the *trans* form is planar, but *cis*-2 is not, the reaction pathway involves not only hydrogen translocation but also the twisting of the two pyrrole units which are protonated in the *cis*-2 form.

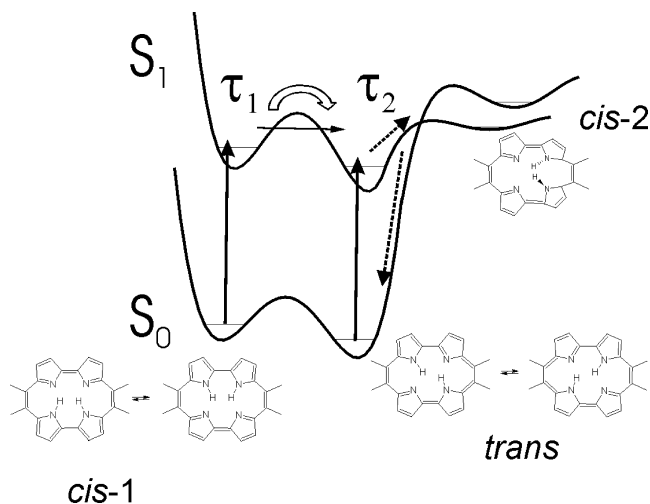


Figure 8. Scheme of excited-state deactivation.

This twisting is facilitated by substitution, e.g., by alkyl groups positioned so that they sterically repel each other. On the other hand, the twisting, a large-amplitude motion, is hindered by increasing solvent viscosity.

The model can thus explain different photophysical behavior of parent Pc and its 2,7,12,17-tetraalkyl-substituted derivatives, which exhibit large and solvent-independent fluorescence quantum yields, and *meso*- or  $\beta,\beta'$ -octaalkylated porphycenes which show strongly viscosity-dependent photophysical behavior. It should be stressed that the barrier to deactivation depends on both intramolecular hydrogen bonding strength and the propensity to undergo deviation from planarity. The fastest deactivation is observed for *meso*-alkylated porphycenes, which have the shortest  $\text{NH}\cdots\text{N}$  distance and thus the strongest hydrogen bond. However, rapid, viscosity-dependent  $S_1$  depopulation is observed also in  $\beta,\beta'$ -octaalkylated porphycenes, for which the  $\text{NH}\cdots\text{N}$  distance is much longer, the hydrogen bond becomes weaker, and the excited-state *trans*–*trans* reaction becomes too slow to be detected at temperatures around 100 K. For these compounds, the ease of twisting is probably the dominant factor.

The results of the present work corroborate the above model by providing quantitative characteristics of  $S_1$  depopulation in two *meso*-tetraalkylated porphycenes carrying different substituents. The deactivation of TMPc is, for each solvent, about 2–3 times faster than the process in TPPc, substituted with more bulky propyl groups. Interestingly, different substituents do not change the strength of intramolecular hydrogen bonds, as can be concluded from the same  $\text{NH}\cdots\text{N}$  distances in the two compounds, 2.53 Å.<sup>9,39</sup> In this context, a very interesting result has been published recently for a new *meso*-substituted derivative, 9,10,19,20-tetraphenylporphycene.<sup>50</sup> The X-ray geometry revealed the same inner cavity dimension as those of TMPc and TPPc. On the other hand, the reported room-temperature fluorescence quantum yield in argon-saturated dichloromethane solution was very high, 0.23. If this result is confirmed, it can provide an example of “rigidization” of a molecule, probably by attractive stacking interactions of phenyl groups.

The model of excited-state deactivation postulates an energy sink along the *trans*–*cis*-2 tautomerization path. In order to explain the mechanism of deactivation in the excited *cis*-1

species, we note that the direct *cis*-1–*cis*-2 conversion does not seem probable. Instead, an excited *cis*-1 structure should tautomerize first to the *trans* species, which then undergoes the depopulation along the *trans*–*cis*-2 coordinate. In order to reconcile this scheme with the experimentally obtained fluorescence kinetics, we attribute the longer decay,  $\tau_2$ , with the dominant amplitude to the *trans* species, and the shorter lifetime,  $\tau_1$ , to the decay of *cis*-1, preferentially to the excited *trans* tautomer (Figure 8). Such assignment, however, has to explain an important observation. Both decay times are found to be sensitive to viscosity, becoming longer in more viscous environments. The model of excited state deactivation presented above can explain the viscosity dependence of excited state *trans*–*cis*-2 reaction, and thus the variation of the longer fluorescence decay component. However, the dependence of *cis*-1–*trans* conversion on viscosity may at first look surprising. A possible explanation is discussed in the next section.

**4.3. Tautomerization Dynamics.** The experimental observation of extremely fast anisotropy decay in TMPc and TPPc demonstrates that the *trans*–*trans* conversion occurs on the time scale of less than 100 fs, both in  $S_0$  and  $S_1$ . On the other hand, the two fluorescence decays are at least 1 or 2 orders of magnitude longer; the difference becomes much larger in more viscous media, where the anisotropy decay is not slowed down, but the emission decay rate is. Moreover, two different lifetimes indicate that no excited-state equilibrium is established. Especially intriguing is that the energetically downhill process, *cis*-1–*trans* conversion is much slower than the *trans*–*trans* tautomerization. In other words, the transfer of two hydrogen atoms, a thermodynamically neutral process is much faster than the translocation of one hydrogen, a reaction with a small, but negative enthalpy. Equally puzzling is the observation that the rate of the single hydrogen transfer process is strongly dependent on viscosity.

In order to explain these phenomena, we start with the conclusions drawn from the supersonic jet work on TMPc and TPPc.<sup>11</sup> The experimentally observed emission intensity pattern could only be explained by assuming that the cross section of the potential energy surface along the hydrogen transfer coordinate is not symmetric, due to the coupling with the rotation of the alkyl groups. This implies that the effective potential barrier for tautomerization “seen” by internal hydrogen atoms depends on the position of the peripheral alkyl groups.

We now further explore this concept by comparing the role of coupling of methyl group rotations with both double hydrogen transfer (*trans*–*trans* and *cis*-1–*cis*-1 processes) and single hydrogen transfer (*cis*-1–*trans* reaction). The positions of methyl substituents were monitored along the possible tautomerization paths and, in particular, at the transition state. The calculations revealed an important difference between the *trans*–*trans* (*cis*-1–*cis*-1) second-order saddle point, with both hydrogens placed in between the nitrogen atoms and the *cis*-1–*trans* transition state, with only one hydrogen being transferred (Figure 9). In the former structure, the methyl groups practically retain their initial positions, whereas in the latter, the two methyl substituents adjacent to pyrrole rings participating in the transfer are twisted by 30 degrees from the initial (and final) locations. It means that *cis*-1–*trans* tautomerization is strongly coupled to the methyl group rotation in the case of a single hydrogen transfer, but not for the double hydrogen transfer. In other words, the effective mass is much larger along the *cis*-1–*trans* path, with possible implications for tunneling probabilities. Most important, the coupling of alkyl torsions with

(50) Anju, K. S.; Ramakrishnan, S.; Thomas, A. P.; Suresh, E.; Srinivasan, A. *Org. Lett.* **2008**, *10*, 5545.



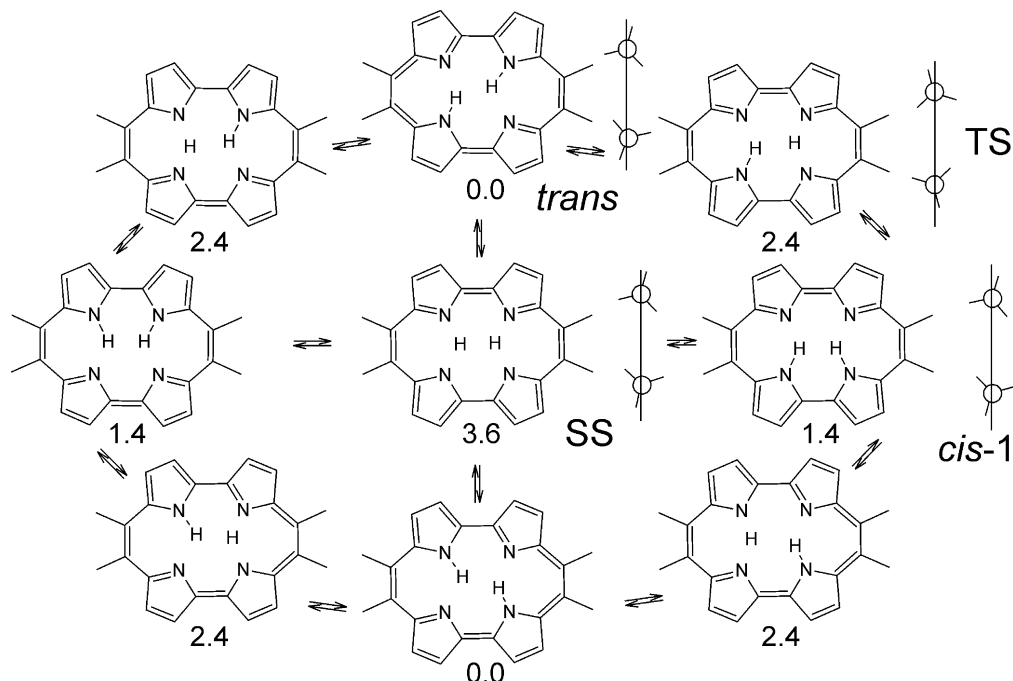


**Figure 9.** Scheme of tautomerization in TMPc with the calculated energy values relative to the ground state (in kcal/mol). The positions of methyl groups are shown in the side views for *trans* and *cis-1* tautomers, as well as for the *cis-1*–*trans* transition state (TS) and for the *trans*–*trans* (or *cis-1*–*cis-1*) second-order saddle point (SS).

single hydrogen transfer can explain the observed viscosity dependence of *cis-1*–*trans* conversion. While the rotation of a single methyl group is a low-barrier process, the close proximity of two methyl groups may lead to substantial barriers and to the sensitivity to the environment. For instance, a barrier as large as 7.8 kcal/mol was observed for methyl rotation in crystalline 1,8-dimethylnaphthalene.<sup>51</sup>

Naturally, a larger barrier is to be expected for TPPc, the porphycene carrying the propyl groups. This is indeed observed experimentally, as can be deduced by comparing the values of the shorter fluorescence decay components in TMPc and TPPc. For the same solvent, the decay in the latter is about twice as long.

We have estimated the barrier associated with two adjacent methyl substituents by calculating the potential energy profiles while rotating each methyl group in steps of 3 degrees; the rest of the molecule was kept rigid (Figure 10). For the ground state, about 1 kcal is required to rotate a methyl group by 30 degrees, in order to obtain the position predicted for the transition state. In fact, this corresponds exactly to the calculated difference between the *cis*–*trans* transition state and the *cis* tautomer (Figure 9), implying that the rotation of methyl substituents is the main coordinate along the *cis-1*–*trans* energy path; this could actually be seen while visually inspecting the changes in nuclear coordinates during optimization to the transition state. Interestingly, the cooperative movement of two methyl groups does not substantially lower this barrier. The picture that emerges is that the *cis-1*–*trans* conversion, involving a single hydrogen transfer is controlled by methyl group rotation. In turn, the methyl torsional motions are influenced by the viscosity of the medium, which explains the experimentally found dependence of the rate on viscosity. One should note that the crucial role of methyl rotation is due to a very low intrinsic barrier for *cis-1*–*trans* tautomerization. For larger barriers, e.g., about 10 kcal/

mol, typical for porphyrins,<sup>52</sup> the energy of the order of 1 kcal/mol would only provide a small correction.

Since our experimental results refer to the viscosity dependence of the *cis-1*–*trans* tautomerization process in *S*<sub>1</sub>, we also attempted to estimate the barrier for this state. A 20 × 20 matrix was obtained by rotating the two methyl substituent in steps of 6 degrees while using the rigid, *S*<sub>1</sub>-optimized geometry. Figure 10 shows that while the overall barrier is lower than for the ground state, the energy required to twist both methyl groups by 30° is actually higher in *S*<sub>1</sub>.

Another factor which should be taken into account in the discussion of coupling of alkyl group torsion with hydrogen transfer is the alternation of single and double character of CC and CN bonds. Sekiya and co-workers discussed this problem for 5-methyltropone<sup>53</sup> and 5-methyl-9-hydroxyphenalenone.<sup>54</sup> In these molecules, hydrogen transfer causes an interchange of double and single bonds formed by carbon to which the methyl group is attached. In the present case, such an effect seems to be of minor importance. Both calculations and the X-ray data for TPPc<sup>39</sup> reveal practically the same lengths, 1.42–1.43 Å for the C8C9, C9C10, and C10C11 (C18C19, C19C20, and C20C1) bonds, which are formally written as single or double. These bonds retain their lengths for the *cis-1*–*trans* transition state (TS) and for the *trans*–*trans* second-order saddle point (SS). Actually, the analysis of overall bond lengths in TS and SS shows larger changes for the latter, with the average change of 0.0087 Å per CC bond in SS compared with 0.0053 Å for TS. These values are an order of magnitude smaller than 0.08

(52) Baker, J.; Kozłowski, P. M.; Jarzecki, A. A.; Pulay, P. *Theor. Chem. Acc.* **1997**, 97, 59.

(53) Nishi, K.; Sekiya, H.; Kawakami, H.; Mori, A.; Nishimura, Y. *J. Chem. Phys.* **1999**, 111, 3961.

(54) Nishi, K.; Sekiya, H.; Mochida, T.; Sugawara, T.; Nishimura, Y. *J. Chem. Phys.* **2000**, 112, 5002.

(51) Wilson, C. C. *Chem. Phys. Lett.* **2002**, 362, 249.

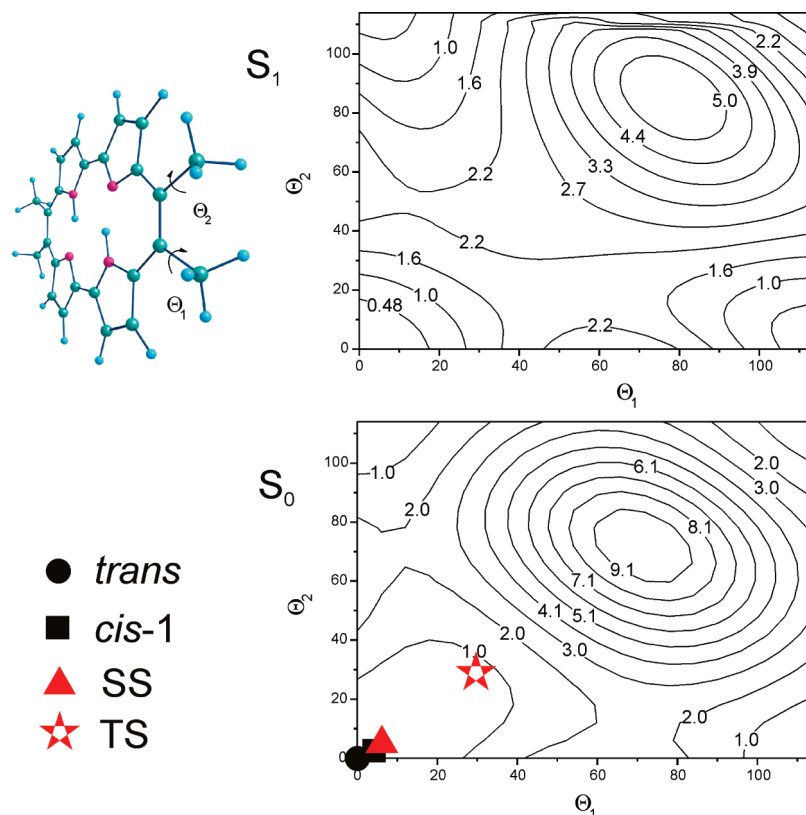


**Figure 10.** Contour plot for the potential energy as a function of rotation of two methyl groups in TMPC, obtained for  $S_0$  (bottom) and  $S_1$  (top). The angles corresponding to the stationary points, computed for  $S_0$ , are also shown. The energies are in kcal/mol.

Å, the difference between CC single and double bonds calculated for tropolone.<sup>55</sup>

To understand better the coupling between the motion of peripheral methyl groups and internal hydrogens, we plan to investigate the derivatives carrying only one methyl group on each ethylene bridge. The initial studies of 2,7-di-*tert*-butyl-10,19-dimethylporphycene show that this molecule is strongly fluorescent even in low viscosity solvents. The finding that the removal of an adjacent alkyl group on the ethylene bridge brings back the radiative properties is another confirmation of the above-presented mechanism of the radiationless deactivation in porphycenes. We emphasize the crucial role of the two excited state *cis* configurations in this mechanism, which is typical of the *meso*-substituted tetraalkylporphycenes and not present in the other porphycene analogues.

Finally, one should point out that a more detailed analysis of molecules with several methyl substituents should extend beyond the simple barrier calculations and take into account quantum mechanical phenomena, such as in-phase or out-of phase motions of the methyl groups.

## 5. Summary and Outlook

*Meso*-substituted tetraalkylporphycenes provide a rare example of porphyrinoids that reveal both *trans* and *cis* tautomeric forms. To the best of our knowledge, no other such porphycene has been found so far. *Cis*-tautomers have been postulated for another porphyrin isomer, octaethylcorphycene, but only for the crystalline form:<sup>56</sup> in solution, the

*trans* form is predominant. For porphyrins, the postulated mechanism for *trans*–*trans* conversion involves thermally activated tunneling to and from the *cis* intermediate, but such a form has never been observed.<sup>57–59</sup>

Studies of the complicated ground- and excited-state tautomeric equilibria involving the *trans* and *cis* structures allow us to elucidate the multidimensional character of tautomerization path. Again, TMPC and TPPC are quite unique, exhibiting the transfer of two hydrogen atoms which is faster than a single particle displacement. Moreover, an “exotic”, twisted *cis* tautomer is postulated to play a crucial role in radiationless deactivation.

All these features make *meso*-substituted porphycenes attractive models for fundamental studies of hydrogen bonding and of such aspects of ground- and excited-state hydrogen transfer as mode-selectivity, coupling between internal modes, tunneling, or cooperativity between two identical hydrogen bonds belonging to the same molecule. Moreover, strongly solvent-dependent photophysics may be an asset in practical applications. One can envisage using the viscosity dependence of the emission for sensing various parts of the cell; such studies seem particularly attractive given that many porphycenes are very good photosensitizers with great potential for photodynamic therapy.<sup>37</sup> In this respect, *meso*-porphycenes are also quite unique, because their oxygen-sensitizing properties should drastically change

(55) Paz, J. J.; Moreno, M.; Lluch, J. M. *J. Chem. Phys.* **1995**, *103*, 353.

(56) Sessler, J. L.; Brucker, E. A.; Weghorn, S. J.; Kisters, M.; Schafer, M.; Lex, J.; Vogel, E. *Angew. Chem., Int. Ed. Engl.* **1994**, *33*, 2308.

(57) Schlabach, M.; Wehrle, B.; Rumpel, H.; Braun, J.; Scherer, G.; Limbach, H. H. *Ber. Bunsen-Ges. Phys. Chem.* **1992**, *96*, 821.

(58) Braun, J.; Schlabach, M.; Wehrle, B.; Köcher, M.; Vogel, E.; Limbach, H. H. *J. Am. Chem. Soc.* **1994**, *116*, 6593.

(59) Braun, J.; Limbach, H. H.; Williams, P. G.; Morimoto, H.; Wemmer, D. E. *J. Am. Chem. Soc.* **1996**, *118*, 7231.

with the viscosity of the environment. Depending on the cellular location, the same molecule may or may not display phototherapeutic activity. The advantages of using such chromophores for studying the mechanisms of phototherapy are obvious.

**Acknowledgment.** This work was supported by Grant No. N204 3329 33 from the Polish Ministry of Science and Higher Education. We acknowledge the computing grant (No. G17-14) from the

Interdisciplinary Centre for Mathematical and Computational Modeling of the Warsaw University.

**Supporting Information Available:** Shapes of frontier molecular orbitals. This information is available free of charge via the Internet at <http://pubs.acs.org/>.

JA105353M